JACS
JOURNAL OF THE AMERICAN CHEMICAL SOCIETY

Article

pubs.acs.org/JACS

Hierarchical Assembly of Cylindrical Block Comicelles Mediated by Spatially Confined Hydrogen-Bonding Interactions

Xiaoyu Li,[†,§,∥] Yang Gao,[†,§] Robert Harniman,[†] Mitchell Winnik,[‡] and Ian Manners*[,†]

[†]School of Chemistry, University of Bristol, Bristol BS8 1TS, United Kingdom

[‡]Department of Chemistry, University of Toronto, Toronto, Ontario M5S 3H6, Canada

Supporting Information

ABSTRACT: Hydrogen bonds are among the most common interactions used by nature for the creation of hierarchical structures from smaller building blocks. Herein, we describe an in-depth study of the hierarchical assembly of cylindrical block comicelles with a crystallizable poly(ferrocenyldimethylsilane) (PFS) core via H-bonding interactions to form complex supermicellar structures. Well-defined block comicelles bearing H-bond donor (H_D) segments (M(PFS-*b*-PMVSOH)), or H-bond acceptor (H_A) segments (M(PFS-*b*-P2VP)), and non-interacting (N) segments (M(PFS-*b*-PtBA)) were created by the living crystallization-driven self-assembly (CDSA) method [PMVSOH = hydroxyl-functionalized poly(methylvinylsiloxane), P2VP = poly(2-vinylpyridine), PtBA = poly(*tert*-butyl acrylate), M = micelle segment]. Due to the control provided by the living CDSA approach, both the block comicelles and the individual segments were virtually monodisperse in length, which facilitated their predictable hierarchical assembly into higher-level structures. Two cases were investigated in detail: first, the interaction of N-H_A-N triblock comicelles with the H_D homopolymer PMVSOH, and second, the interaction of N-H_D-N triblock comicelles with very short H_A cylinders (seeds). By manipulation of several factors, namely coronal steric effects (via the PtBA corona chain) and attractive interaction strength (via the H-bonding interaction between P2VP and PMVSOH), the aggregation of the triblock comicelles could be controlled, and well-defined multi-micrometer-size structures such as "shish-kebab"-shaped supermicelles were prepared. The ability of the seeds adsorbed on the block comicelles to function as initiators for living CDSA to generate fence-like "shish-kebab" superstructures was also explored.

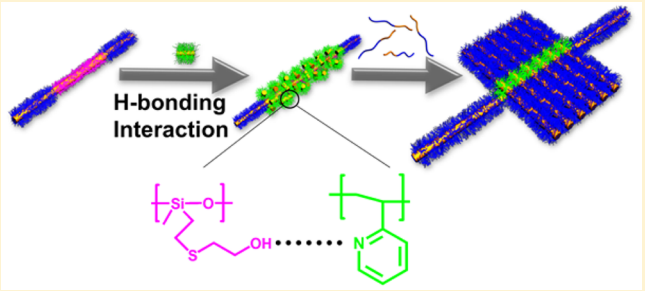

1. INTRODUCTION

Nature's biological diversity relies on multi-tier self-assembly based on weak non-covalent interactions such as electrostatic, hydrogen-bonding, and hydrophobic forces.[1] A classic example is provided by the interstrand H-bonds that stabilize the double-helical structure of DNA, an essential element for genetics.[2] Furthermore, for polypeptides, the precise positioning of the H-bonding segments is of crucial importance for the correct folding and thus the function of proteins.[3] Inspired by Nature, scientists have utilized the H-bonding interaction to direct the assembly of artificial materials into higher-level structures.[4] For example, the specific H-bond interactions between the DNA base-pairs have been used to direct the assembly of synthetic DNA molecules into highly regulated and exquisitely controlled architectures ("DNA origami").[5] In synthetic materials, H-bonding interactions between small molecules,[6] polymer/small molecule pairs,[7] and polymer/polymer pairs[8] have been extensively exploited to create higher-level structures.

Self-assembly of block copolymers (BCPs) is an efficient bottom-up approach to create nanoscopic structures with complex architectures and multiple functionalities.[9] However, only a few examples have been reported on the hierarchical self-assembly of BCP micelles to form supermicellar micrometer-scale structures, and these have involved the utilization of electrostatic[10] or amphiphilic interactions.[9c,d,11] The use of H-bond donor−acceptor binding is an appealing approach, but difficulties are anticipated concerning tuning of the strength of the interaction and the precise positioning of the interacting segments to produce well-defined supermicelles. Moreover, to avoid the buildup of defects from the formation of undesirable kinetically trapped structures, hierarchical assembly requires robust building blocks of near-identical size and periodicity and some degree of dynamic character to the interactions. In cases where the structures can be precisely controlled, spherical Janus and patchy particles based on BCPs have been shown to be very useful building blocks.[9c,d,11]

Among the examples of hierarchical assembly of BCP micelles, the case of cylinders is particularly interesting. Similar structures are able to resemble the assembly of collagen fibrils to form the main scaffold in bone.[1] For example, a synthetic collagen mimic polypeptide has been shown to assemble into nanofibers, which can further hierarchically assemble to form hydrogels.[12] Similarly, Janus cylinders made from synthetic BCPs can aggregate through well-defined solvophobic regions

Received: June 19, 2016
Published: August 23, 2016

DOI: 10.1021/jacs.6b05973
J. Am. Chem. Soc. 2016, 138, 12902−12912

Scheme 1. Chemical Structures of Polymers, Schematic Representations of Triblock Comicelles (I), and Their Hierarchical Assembly via H-Bonding Interactions (II)

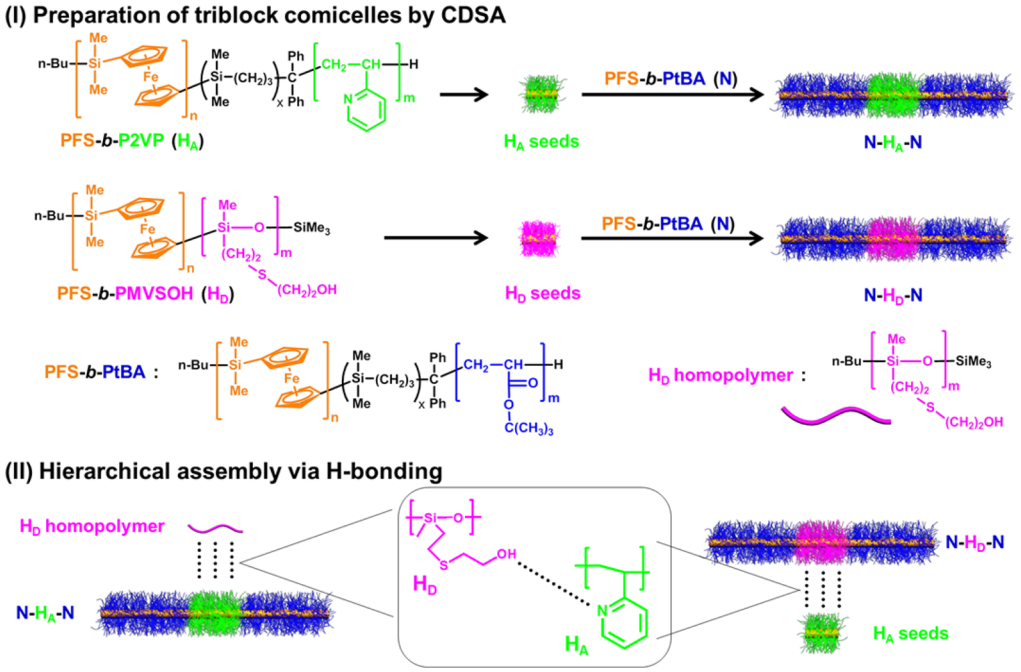

in selective solvents to form cylindrical bundles.[11c] Composite cylindrical structures have been formed by mixing two oppositely charged cylinders[10c] or cylinders and spheres,[10a,b] and the generation of well-defined hierarchical structures from amphiphilic cylindrical micelles has recently been achieved.[11a,e]

We have previously shown that BCPs with a crystallizable poly(ferrocenyldimethylsilane) (PFS) core-forming block can self-assemble into cylindrical micelles in selective solvents for the corona-forming block. Significantly, the termini of the crystalline PFS micelle core remain active to further growth via a process termed living crystallization-driven self-assembly (CDSA).[13] Following sonication to form short seeds, relatively monodisperse cylinders (L_w/L_n < 1.1, where L_w and L_n are weight- and number-average lengths, respectively) with controlled lengths from ca. 40 nm to 2 μm have been obtained using this living CDSA approach by variation of the unimer-to-seed ratio.[14] It is also possible to generate complex micelle architectures with segmented coronas, including multi-block comicelles such as monochrome and multi-color fluorescent "barcode",[13a,15] multi-armed micelles,[16] and non-centrosymmetric structures.[17] The living CDSA process has also been extended to BCPs containing other crystallizable core-forming blocks, including polylactide,[18] poly(3-hexylthiophene),[19] and polyethylene,[20] as well as to two dimensions.[21]

Block comicelles prepared by the living CDSA method possess precisely controllable dimensions and coronal chemistries and are ideal candidates for higher-level assembly. Amphiphilic triblock comicelles can be assembled into multidimensional structures in selective solvents.[11a,e,22] Recently, we reported the synthesis of complex "windmill-like" supermicelles by combining H-bonding interactions and segment solvophobicity of triblock comicelles.[23] We also demonstrated that, when mixing two kinds of block comicelles containing a H-bond donor or acceptor region together with non-interactive segments, linear or "I"-shaped supermicelles[23] or "cross"-like supermicelles[22b,23] can be formed by controlling the location of the confined of the H-bond donor/acceptor segments. Herein, as a follow up to a communication in which we reported some preliminary results,[23] we describe an in-depth systematic study of the hierarchical assembly of triblock comicelles with homopolymer or short cylinder seeds using H-bond interactions. The work demonstrates the formation of complex supermicelle architectures from building blocks created by living CDSA. In particular, we focus on the interaction of the block comicelles with homopolymers or short seeds via H-bonds to yield composite supermicelles with "shish-kebab" architectures.

2. RESULTS

For the systematic study of the triblock comicelle assembly, three kinds of BCPs were used (Scheme 1): a H-bond donor (H_D) segment-forming BCP, PFS-*b*-PMVSOH (PMVSOH = hydroxyl-functionalized poly(vinylmethylsiloxane)); a H-bond acceptor (H_A) segment-forming BCP, PFS-*b*-P2VP (P2VP = poly(2-vinylpyridine)); and a non-interacting (N) segment-forming BCP, PFS-*b*-PtBA (PtBA = poly(*tert*-butyl acrylate)). All BCPs were prepared by sequential living anionic polymerization,[24] and all contain a crystallizable PFS core-forming block.[25] Also used was an H_D homopolymer PMVSOH, which was obtained via functionalization of PMVS by thiol−ene click chemistry.[26] The characterization of all the polymers is included in Table S1.

For convenience, as the crystalline PFS core was a common feature, all of the triblock comicelles are depicted in an abbreviated form that reflects their coronal chemistry. For example, triblock comicelle M(PFS_{20}-*b*-$PtBA_{280}$)-*b*-M(PFS_{20}-*b*-$P2VP_{448}$)-*b*-M(PFS_{20}-*b*-$PtBA_{280}$), with a central M(PFS_{20}-*b*-$P2VP_{448}$) segment of 50 nm in length, is described as N_{280}-$H_{A,448}$(50 nm)-N_{280}. The subscript numbers represent the degree of polymerization (DP) of the corona-forming block. The length in the parentheses is that of the central (in this case H_A) segment. For H_D segments used in the current study, since

DOI: 10.1021/jacs.6b05973
J. Am. Chem. Soc. 2016, 138, 12902−12912

only one diblock copolymer, PFS_{20}-*b*-$PMVSOH_{120}$, is used, the H_D segments are all described as $H_{D,120}$. As we discussed previously,[22b] the length of soluble corona chains (or corona layer thickness) of PtBA or P2VP is greatly dependent on the DP of PtBA or P2VP blocks, respectively. Thus, herein we will use DP_{PtBA} or DP_{P2VP} as an indication of the length of the corona PtBA or P2VP chains, respectively.

The triblock comicelles, for example, N-H_D-N cylinders, were prepared by seeded growth from short H_D cylindrical micelles (seeds) via living CDSA (Scheme 1(I)). First, low-dispersity H_D micelle seeds were prepared by the addition of PFS_{20}-*b*-$PMVSOH_{120}$ unimers in THF to a solution of small PFS_{20}-*b*-$PMVSOH_{120}$ crystallites in isopropanol (*i*-PrOH) (ca. 50 nm in length, prepared by sonication of long cylindrical micelle precursors). The length of the H_D micelle seeds was controlled by the ratio of the PFS_{20}-*b*-$PMVSOH_{120}$ unimers to the small crystallites (see Table S2). To the *i*-PrOH solution of the H_D seeds was added the desired amount of PFS-*b*-PtBA unimers in a small portion of THF to achieve the desired N-H_D-N cylinder length. N-H_A-N triblock comicelles were prepared in an analogous manner from H_A seeds. All the seed cylinders and triblock comicelles were characterized by transmission electron microscopy (TEM). As can be appreciated from the TEM images and summarized data (Tables S2 and S3, Figures S1–S4), both seeds and triblock comicelles were uniform in length, due to the control arising from the living CDSA method. This ensured that all the micelles from the sample possessed a very similar structure, a feature likely to facilitate their controlled hierarchical assembly.

Two approaches to the hierarchical assembly of the cylindrical block comicelles have been explored in this study. These are illustrated in Scheme 1(II). The first involves the assembly of triblock comicelles (N-H_A-N) through H-bonding with H_D homopolymer (PMVSOH) and the second, triblock comicelles (N-H_D-N) with short cylindrical seeds (H_A).

2.1. Interactions between H_D Homopolymer and H_A Short Cylinder Seeds: Formation of Precipitates. Over the past few decades, H-bonding interactions have been widely used to prepare non-covalently linked BCPs, for layer-by-layer assembly, and to induce the micellization of BCPs.[27] However, if no spatial confinement is introduced, the hierarchical assembly of BCP micelles via H-bonding usually leads to precipitates in solution due to the abundant complementary interactive sites among different chains to form "H-bond networks".[27a,28] Similarly, when H_D homopolymer $PMVSOH_{105}$ and $H_{A,448}$ seeds (ca. 50 nm) were mixed in *i*-PrOH (a selective solvent for PtBA, PMVSOH and P2VP blocks), precipitates were observed in 30 s (hydroxyl/pyridyl mole ratio = 1/1), and large aggregates could be observed by TEM (Figure S5c). Meanwhile, at other mole ratios, the solutions turned cloudy, and small aggregates were observed by TEM (Figure S5). The formation of these aggregates is attributed to the presence of H-bonding interactions between the hydroxyl and pyridyl groups of PMVSOH and P2VP, respectively, as demonstrated in our preliminary communication using FTIR spectroscopy.[23]

2.2. Interactions between H_D Homopolymer and Triblock Comicelle N-H_A-N: Formation of "Shish-kebab" Structures. Based on these observations, next we investigated the more controlled interactions between the H_D homopolymer, PMVSOH, and N-H_A-N triblock comicelles, in which the H_A polymer chains were confined to the corona of the central segment of the cylindrical micelle building block (Figure 1e). The N segments are non-interactive with other segments and were anticipated to act as shielding segments to

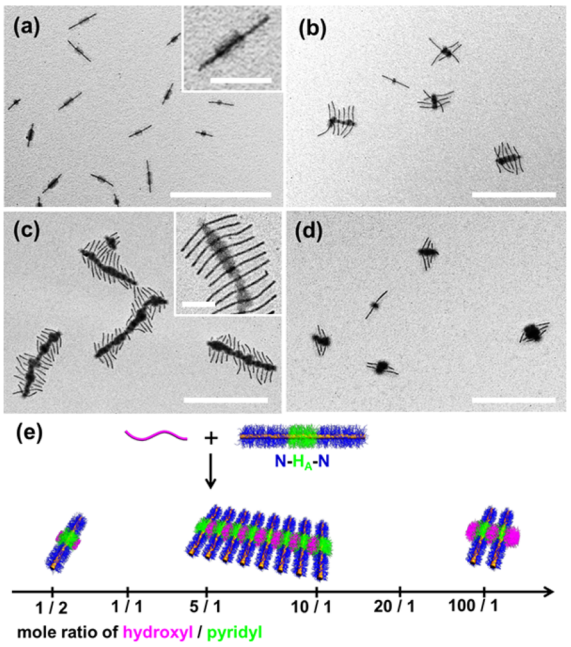

Figure 1. TEM images (a–d) and schematic illustration (e) of the assemblies obtained by mixing H_D homopolymer $PMVSOH_{105}$ and N_{280}-$H_{A,448}$(50 nm)-N_{280} with a hydroxyl/pyridyl mole ratio of (a) 1/2, (b) 1/1, (c) 5/1, and (d) 100/1 (final concentration of H_A segment is 0.02 mg/mL). Scale bars are 1 μm, and 200 nm in the insets.

increase the colloidal stability of the resulting supermicellar structures. Indeed, TEM analysis showed that addition of an *i*-PrOH solution of H_D homopolymer to the *i*-PrOH solution of the triblock comicelle N_{280}-$H_{A,448}$(50 nm)-N_{280} at a mole ratio of hydroxyl/pyridyl groups of 5/1 led to assembly of the comicelles through the central H_A coronal segments in a parallel fashion, forming "shish-kebab" supermicelles (Figure 1c and Figure S6c,d). The H_D homopolymer chains functioned as a "glue" to enable the assembly of triblock comicelles via H-bonding interactions. By varying the mole ratio of hydroxyl/pyridyl groups through the series from 1/2 to 1/1, 5/1, 10/1, 20/1, and 100/1, it was established that the "shish-kebab" supermicelles were formed only at hydroxyl/pyridyl ratios from 5/1 to 20/1. Meanwhile, the use of either a very low or very high mole ratio of hydroxyl/pyridyl groups led to a significant reduction of the aggregation number (or arm distribution) in each supermicelle (Figure 1 and Figure S6). On the other hand, our experimental results suggested that concentration did not have a significant effect on the morphology of the supermicelles (see Figure S7).

We envisage that the final supermicelle structures formed are the result of competing effects arising from attractive H-bonding interactions between H_A and H_D and repulsive forces between the N corona chains due to steric hindrance. By using different BCPs or different block comicelle segment lengths, the strengths of the attractive or repulsive interactions can be tuned, and thus different supermicelles can be obtained. To verify this postulate, in the following experiments we tuned the respective interaction energies by using P2VP or PtBA with different DP values for the H_A and N segments, respectively, and different segment lengths of H_A and N in the triblock comicelle.

DOI: 10.1021/jacs.6b05973
J. Am. Chem. Soc. 2016, 138, 12902–12912

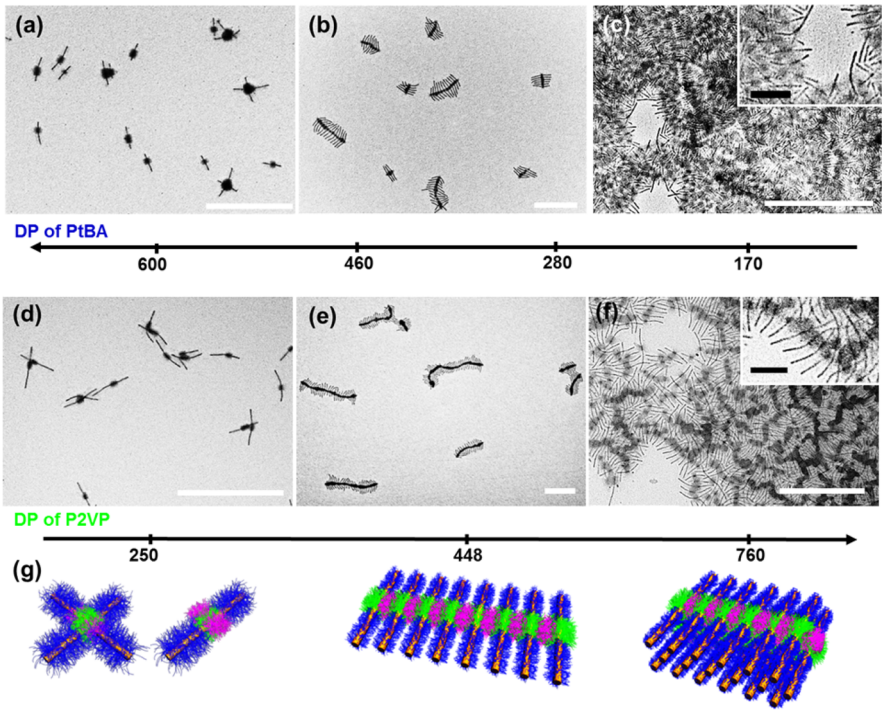

Figure 2. TEM images of the supermicelle structures formed by H_D-homopolymer $PMVSOH_{105}$ with (a–c) N-$H_{A,448}$-N cylinders with DP_{PtBA} = (a) 600, (b) 460, and (c) 170, and with (d–f) N_{280}-H_A-N_{280} cylinders with DP_{P2VP} = (d) 250, (e) 448, and (f) 760. Hydroxyl/pyridyl mole ratio = 5/1, and final concentration of H_A segments = 0.02 mg/mL. The aggregation in the case of (c) leads to much more tightly packed comicelles than in the case of (f), which leads to poorer resolution of the individual structures. Scale bars are 1 μm in the images and 200 nm in the insets. (g) Schematic illustrations of the supermicelle structures of (from left to right) "dimers" and individual block comicelles, "shish-kebab" supermicelles, and large three-dimensional aggregates formed by varying the DP of the PtBA and P2VP blocks.

To investigate the steric hindrance effects that arise from the corona chains of the N segments on supermicelle formation, four triblock comicelles N-$H_{A,448}$(50 nm)-N with the same H_A segments and different N segments with DP_{PtBA} = 600, 460, 280, and 170 were prepared (from four different N segment-forming PFS-*b*-PtBA diblock copolymers, see Table S1). The triblock comicelles were mixed with same H_D homopolymer $PMVSOH_{105}$ at hydroxyl/pyridyl mole ratio = 5/1 in *i*-PrOH.

TEM results showed that when DP_{PtBA} = 600 (Figure 2a), the triblock comicelles either remained as individual entities or only formed "dimers" with two triblock comicelles attached to one another. In contrast, when DP_{PtBA} = 460 (Figure 2b) and 280, "shish-kebab" supermicelles were formed (Figure 1c). Furthermore, when DP_{PtBA} = 170, the triblock comicelles formed large aggregates with three-dimensional structures (Figure 2c; additional low-resolution TEM images of the superstructures are included in Figure S8).

Similarly, the strength of the attractive H-bonding interactions could be tuned by using H_A segment-forming diblock copolymers with different numbers of H-bonding sites. Superstructures were prepared from three different triblock comicelles N_{280}-H_A(50 nm)-N_{280} with similar N segments (corona chain length DP_{PtBA} = 280 and N segment length = 100–200 nm) but different values of DP_{P2VP}. Under the same experimental conditions, after the addition of H_D homopolymer, $PMVSOH_{105}$, the triblock comicelles formed only "oligomers" (aggregates of 1–3 micelles) when DP_{P2VP} = 250 (Figure 2d), but they formed "shish-kebab" supermicelles when DP_{P2VP} = 448 (Figure 2e). Large three-dimensional aggregates were observed when DP_{P2VP} = 760 (Figure 2f; additional TEM images of the superstructures are included in Figure S9).

An alternative method with which to strengthen the attractive interaction is to increase the length of the H_A segments. Three different triblock comicelles N_{280}-$H_{A,448}$-N_{280}, with a similar N segment length = 100–200 nm and different lengths for the H_A segment (50, 190, and 380 nm) were therefore prepared and studied. Upon addition of H_D homopolymer, all three samples gave supermicelles with structures based on parallel-packed triblock comicelles; however, key differences were observed (Figure 3). When the H_A segment was short (50 nm), only "shish-kebab" supermicelles were formed, the triblock comicelles were packed side-by-side, and the supermicelles were elongated only in one direction (Figures 1c, 2e, and 3a). However, when the length of the H_A segment increased to 190 nm, the triblock comicelles were not only able to pack in a parallel fashion in one direction but also in three dimensions (Figure 3b), forming multi-layered bundles. When the length of the H_A segment was further increased to 380 nm, the size of the supermicelles was greatly increased (Figure 3c,d), and a multi-layered bundle structure is clear in the inset image (for additional TEM images see Figure S10).

In contrast, increasing the length of the N segments did not significantly change the morphology of the resultant supermicelles. As shown in Figure 4a,b and Figure S11a–c, three different triblock comicelles, N_{280}-$H_{A,760}$(50 nm)-N_{280}, N_{280}-$H_{A,448}$(50 nm)-N_{280}, or N_{170}-$H_{A,448}$(50 nm)-N_{170}, with longer N segments (450 nm) were used to replace those used in the previous set of experiments where the length of the N segment was around 100–200 nm. Similar "shish-kebab" supermicelles were observed. When the two kinds of N_{280}-$H_{A,448}$(50 nm)-N_{280} triblock comicelles (length of N segments = 150 and 450 nm,

DOI: 10.1021/jacs.6b05973
J. Am. Chem. Soc. 2016, 138, 12902–12912

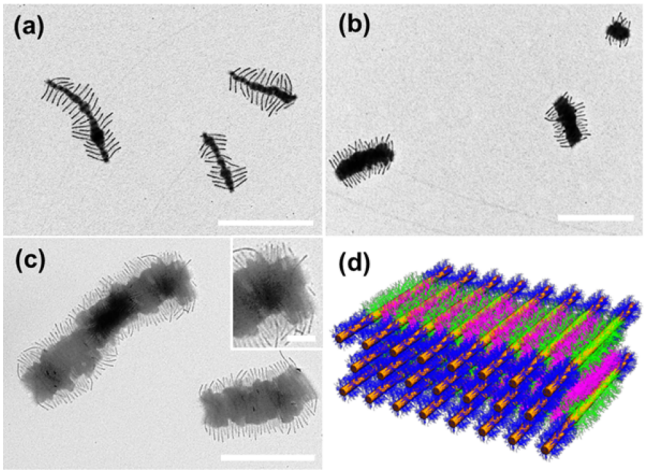

Figure 3. TEM images of supermicellar structures prepared by mixing H_D homopolymer $PMVSOH_{105}$ and N_{280}-$H_{A,448}$-N_{280} with hydroxyl/pyridyl mole ratio = 5/1, final concentration of H_A segments = 0.02 mg/mL, and length of H_A segment = (a) 50, (b) 190, and (c) 380 nm. Scale bars are 1 μm, and 200 nm in the inset. (d) Schematic illustration of the large three-dimensional supermicelle structures shown in image (c).

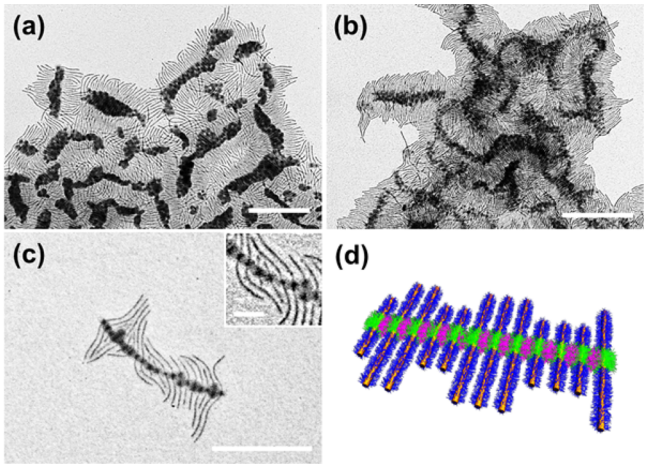

Figure 4. TEM images of "shish-kebab" superstructures prepared by mixing H_D homopolymer $PMVSOH_{105}$ with (a) N_{280}-$H_{A,760}$(50 nm)-N_{280} (N segment length = 450 nm), (b) N_{170}-$H_{A,448}$(50 nm)-N_{170} (N segment length = 450 nm), and (c) mixtures of N_{280}-$H_{A,448}$(50 nm)-N_{280} triblock comicelles with N segment length = 450 and 150 nm, hydroxyl/pyridyl mole ratio = 5/1, and final concentration of H_A segments = 0.02 mg/mL. Scale bars are 1 μm for the images and 200 nm for the insets. Shown in (d) is the schematic illustration of the superstructures shown in (c).

respectively) were mixed in *i*-PrOH, after the addition of H_D homopolymer, $PMVSOH_{105}$, "shish-kebab" supermicelles were also formed, but with alternating long and short triblock comicelles, as shown in Figure 4c,d and Figure S11d.

We also measured the apparent hydrodynamic diameter of the initial triblock comicelles N_{280}-$H_{A,448}$(50 nm)-N_{280} (with N segment length = 450 nm) and the corresponding "shish-kebab" supermicelles via dynamic light scattering experiments (DLS) (Figure S12). The apparent hydrodynamic diameter of the triblock comicelles N_{280}-$H_{A,448}$(50 nm)-N_{280} (with N segment length = 450 nm) increased from 230 to 615 nm after the addition of H_D homopolymer $PMVSOH_{105}$. This increase in apparent hydrodynamic size is clearly consistent with the formation of "shish-kebab" supermicelles in solution rather than during solvent removal on drying. The result is also consistent with our previous characterization of supermicelle formation in solution using non-covalent interactions by laser scanning confocal fluorescence microscopy (LSCFM).[11e,23]

2.3. Interactions between Triblock Comicelles N-H_D-N and H_A Seeds: Formation of Composite "Shish-kebab" Supermicelles and Fence-like "Shish-kebab" Supermicelles. Next, we investigated the hierarchical assembly behavior of N-H_D-N triblock comicelles and H_A seeds at various hydroxyl/pyridyl mole ratios (Figure S13). It was revealed by TEM analysis that excess pyridyl groups were necessary (hydroxyl/pyridyl mole ratio = 1/2, Figure S13b) for discrete composite block comicelles to be formed. The resulting structures possessed H_A seeds attached to the surface of the central H_D segments and resembled the composite "shish-kebab" structure. The presence of a small number of free H_A seeds was also detected. The yields of each kind of supermicelle in this study are summarized in Table S4.

We then explored the analogous assembly process for N_{280}-$H_{D,120}$-N_{280} triblock comicelles and H_A seeds where the latter were made from different PFS-*b*-P2VP diblock copolymers. Three kinds of H_A seeds, $H_{A,250}$, $H_{A,448}$, and $H_{A,760}$, with different DP values for the P2VP block but of similar length (ca. 50 nm) were separately added into the *i*-PrOH solution of N_{280}-$H_{D,120}$(600 nm)-N_{280} triblock comicelles, and the TEM images of the resulting supermicelles are shown in Figure 5.

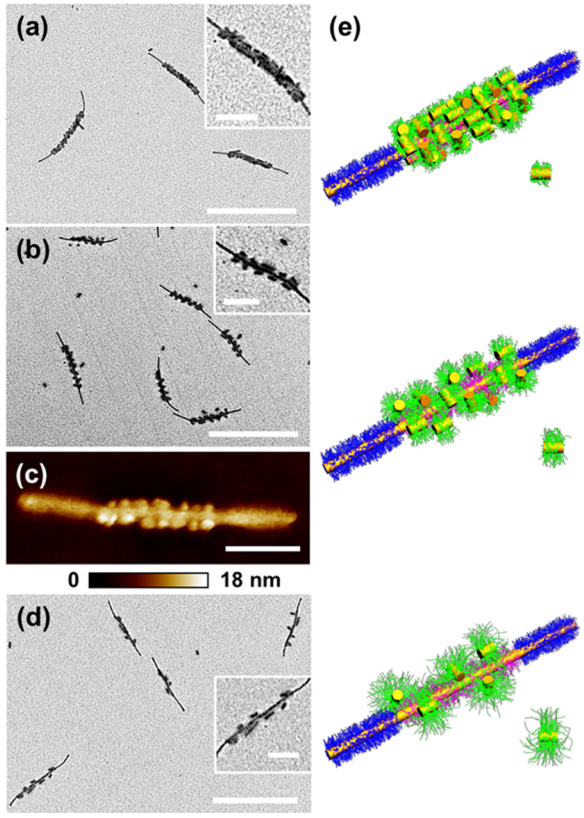

Figure 5. TEM images (a,b,d), AFM height image (c), and schematic illustrations (e) of composite "shish-kebab" structure from N_{280}-$H_{D,120}$(600 nm)-N_{280} triblock comicelles with (a) $H_{A,250}$ seeds, (b,c) $H_{A,448}$ seeds, and (d) $H_{A,760}$ seeds (all the seeds had lengths of ca. 50 nm; see Table S2 and Figure S2). Hydroxyl/pyridyl mole ratio = 1/2. Scale bars are 2 μm, and 200 nm in the inset and AFM images.

DOI: 10.1021/jacs.6b05973
J. Am. Chem. Soc. 2016, 138, 12902−12912

Interestingly, the number of H_A seeds that could be adsorbed onto the triblock comicelles varied significantly. With an increasing DP value for the P2VP block in the H_A seed, the number of adsorbed seeds decreased, as illustrated in the scheme in Figure 5e.

A possible explanation for this phenomenon starts from the assumption that increasing the DP value for the P2VP block in the H_A seed provides more H-bonding accepting sites. Therefore, fewer seeds are needed to bind to the existing H-bond donating sites in the central H_D segments of the N_{280}-$H_{D,120}$(600 nm)-N_{280} triblock comicelles. A steric effect may also play a role, and a significant increase in hydrodynamic size for the H_A seeds in solution with an increase in the DP value of the P2VP was detected by DLS analysis (Figure S15). Thus, with an increasing DP value for the P2VP block, even though the lengths of seeds appeared to be very similar (ca. 50 nm, Figure S2), their increasing hydrodynamic diameters in solution would be expected to lead to a decreasing number of H_A seeds adsorbed. An AFM height image of the composite "shish-kebab" supermicelles from N_{280}-$H_{D,120}$-N_{280} triblock comicelles and $H_{A,448}$ seeds was obtained (Figure 5c), and it can be clearly observed that the $H_{A,448}$ seeds were attached only on the central H_D segments. A cross-sectional analysis (Figure S16) showed that the central H_D segments with the adsorbed H_A seeds were similar in height to the individual N segments. It appears in the AFM image that the H_A seeds were distributed only on the two edges of the H_D segment (Figure 5c). This could be explained by the fact that the H_A seeds and H_D segments were attached by the interaction between their corona chains, which permits appreciable freedom for the seeds to move around when the supermicelles are dried on a substrate.

In the next set of experiments, triblock comicelles N_{280}-$H_{D,120}$-N_{280} with different lengths for the H_D segments (610 nm, 880 nm, and 3.2 μm) were mixed with $H_{A,448}$ seeds in *i*-PrOH at a hydroxyl/pyridyl mole ratio = 1/2. The lengths of the H_D segments were uniform and precisely controlled via living CDSA (Figure S3). Composite "shish-kebab" structures were observed by TEM (Figure 6a,b and Figure S14a–c), and the H_D segments were fully covered by H_A seeds.

The bound H_A seeds were found to be still active to living CDSA,[23,29] and addition of the PFS-*b*-PtBA unimers led to the formation of new N segments (Figure 7e). Interestingly, the subsequent growth of the N segments led to their mutual repulsion and resulted in a perpendicular alignment of the N-H_D-N comicelles relative to the cross supermicelle arms. This afforded hierarchical fence-like "shish-kebab" supermicelles with high uniformity in size, architecture, and yield (Figure 7a–c and Figure S14d–f). An AFM height image (Figure 7d and Figure S17) was also obtained from the same sample. A cross-sectional analysis (Figure S17c) showed that the height of the central section of the supermicelles was around 30 nm, three times that of the individual N segments. This suggests that the N segments, which were grown from the H_A seeds, were distributed on both upper and lower sides of the N-H_D-N triblock comicelles. It is noteworthy that the added unimers grow not only from the termini of seeds but also from the ends of the original triblock comicelles, resulting in an increase in the overall length of the supermicelles.

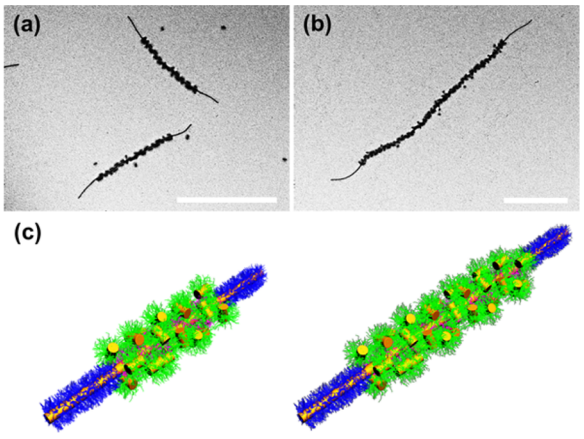

Figure 6. TEM images (a,b) and schematic illustration (c) of composite "shish-kebab" supermicellar structures prepared by mixing $H_{A,448}$ seeds (50 nm, L_w/L_n = 1.1) with N_{280}-$H_{D,120}$-N_{280} cylinders. The lengths of H_D segments are (a) 880 nm and (b) 3.2 μm. Mole ratio of hydroxyl/pyridyl = 1/2. Scale bars are 1 μm.

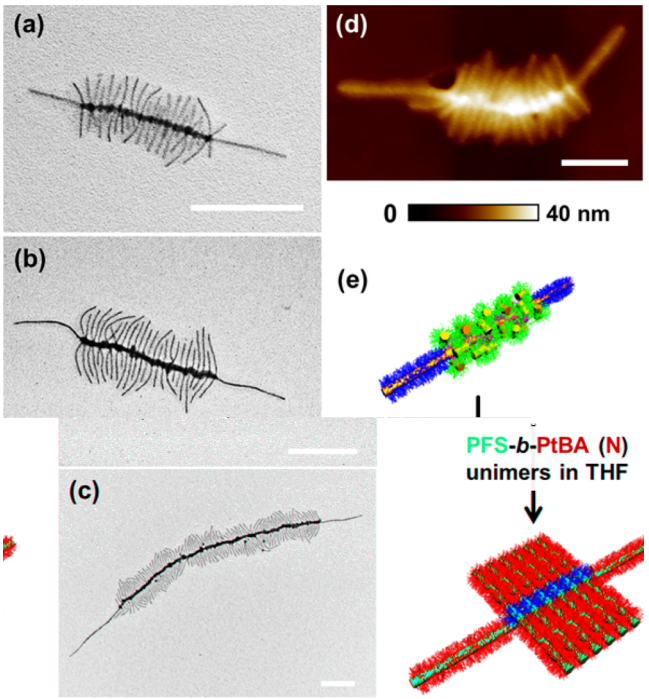

Figure 7. TEM images (a–c), AFM height image (d), and schematic illustrations (e) of fence-like "shish-kebab" superstructures formed by adding PFS_{20}-*b*-$PtBA_{280}$ unimers to the previous "shish-kebab" structure solutions in Figure 6. The lengths of H_D segments are (a) 600 nm, (b) 880 nm, and (c) 3.2 μm. Scale bars are 500 nm in (a–c) and 200 nm in (d).

Direct characterization of the supermicelles in solution was achieved using LSCFM analysis of fence-like "shish-kebab" supermicelles with N segments labeled with red fluorescent BODIPY dyes.[23] Red dye-labeled N segments were grown from the H_A seeds by living CDSA. A LSCFM image of the fluorescent fence-like "shish-kebab" supermicelles in *i*-PrOH solution is shown in Figure S18a. The N-segments grown on the fence-like "shish-kebab" supermicelles appear to be randomly oriented in the solution state, as shown in Figure S18b, instead of being coplanar as found by TEM. This can be best appreciated from the fuzzy edge of the supermicelles in the LSCFM images. This presumably plays a significant role in preventing further aggregation of the structures in solution.

DOI: 10.1021/jacs.6b05973
J. Am. Chem. Soc. 2016, 138, 12902–12912

Taking advantage of living CDSA, we were able to successfully prepare heptablock comicelles N_{280}-$H_{D,120}$(500 nm)-N_{280}-$H_{D,120}$(3.2 μm)-N_{280}-$H_{D,120}$(500 nm)-N_{280}. The length of each of the segments was precisely controlled. When H_A seeds in *i*-PrOH were added, they were adsorbed onto the H_D segments and formed heptablock fence-like "shish-kebab" supermicelles (Figure 8a,c). The addition of PFS-*b*-PtBA unimers led to the formation of heptablock fence-like "shish-kebab" supermicelles after overnight aging at 23 °C, as shown in Figure 8b,d. Interestingly, when the heptablock fence-like "shish-kebab" supermicelles were characterized 20 min after the addition of PFS-*b*-PtBA unimers, not all the unimers had been consumed and grown into N segments from the H_A seeds. As shown in Figure S19a,b, the new N-H_A-N triblock comicelles with short N segments were closely attached to the H_D segments of the heptablock, clearly demonstrating the growth of the N segments.

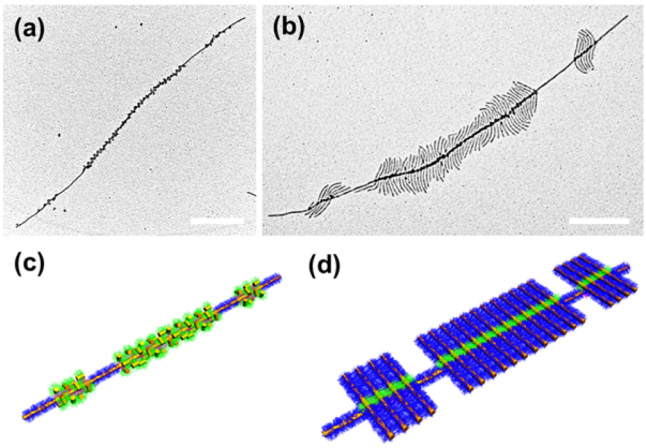

Figure 8. (a,b) TEM images and (c,d) schematic illustrations of (a,c) heptablock composite "shish-kebab" supermicelles prepared by mixing $H_{A,448}$ seeds (50 nm) with N_{280}-$H_{D,120}$(500 nm)-N_{280}-$H_{D,120}$(3.2 μm)-N_{280}-$H_{D,120}$(500 nm)-N_{280} heptablock comicelles and (b,d) block fence-like "shish-kebab" supermicelles prepared by adding PFS_{20}-*b*-$PtBA_{280}$ unimers to the previous "shish-kebab" structure. Scale bars are 1 μm.

Lastly, from TEM images, we measured the length of the H_D segments in the N-H_D-N triblock comicelles and also counted the number of $H_{A,448}$ seeds that could be adsorbed. Over 300 "shish-kebab" supermicelles were measured, and the data are plotted in Figure 9a. From the plots, we could calculate the average length occupied by each $H_{A,448}$ seed to be 38 nm. However, when N_{280}-$H_{D,120}$(50 nm)-N_{280} triblock comicelles were used, no seed attachment was detected, and solely a mixture of the seeds and triblock comicelles was obtained (Figure S20). Only when the length of H_D segments was increased to about 80 nm were the $H_{A,448}$ seeds able to be adsorbed onto the N_{280}-$H_{D,120}$(80 nm)-N_{280} triblock comicelles (Figure 9b). However, instead of forming a one-to-one complex, two $H_{A,448}$ seeds adsorbed onto each N_{280}-$H_{D,120}$(80 nm)-N_{280} triblock comicelle (as can be seen clearly from the inset image in Figure 9b). A schematic illustration of this process is included in Figure 9d. After the addition of PFS_{20}-*b*-$PtBA_{280}$ unimers, new N segments were grown from the two $H_{A,448}$ seeds, as shown in Figure 9c.

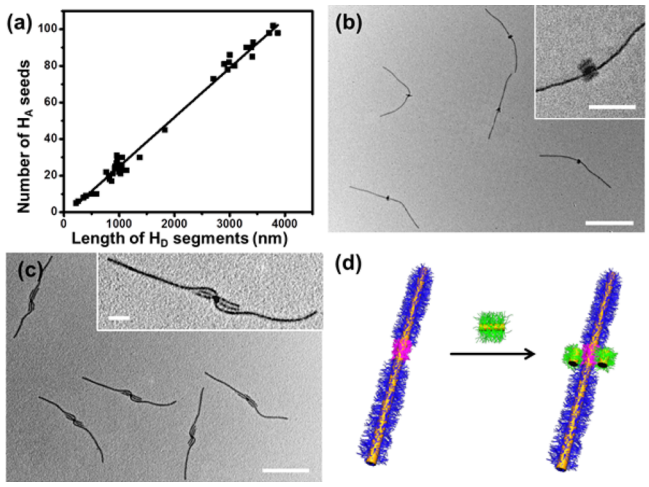

Figure 9. (a) Plot of length of H_D segments versus the number of $H_{A,448}$ seeds that can be adsorbed onto the triblock comicelles (the dashed line is the linear fit of these data points). (b) TEM images of the supermicelles prepared by mixing $H_{A,448}$ seeds (50 nm) with N_{280}-$H_{D,120}$(80 nm)-N_{280} triblock comicelles. Hydroxyl/pyridyl ratio = 2/1. Shown in image (c) are the supermicelles obtained after adding PFS_{20}-*b*-$PtBA_{280}$ unimers to the sample shown in image (b). Schematic illustrations of these supermicelle samples are included in (d). Scale bars are 1 μm for the images and 200 nm for the insets.

3. DISCUSSION

3.1. Effect of Mole Ratios of Hydroxyl/Pyridyl Groups.

It is noteworthy that, in the three hierarchical assembly cases explored in this study (H_D PMVSOH homopolymer with H_A seeds, H_D PMVSOH homopolymer with N-H_A-N triblock comicelles, and N-H_D-N triblock comicelles with H_A seeds), the optimum mole ratios of hydroxyl/pyridyl groups (i.e., the ratio at which the yield of supermicelles was maximized) are different. For the case of H_D PMVSOH homopolymer and H_A seeds, the largest amount of precipitate was formed when the ratio was 1/1, suggesting that the full binding of all the interacting sites was optimum for the formation of aggregates. On the other hand, in the case of H_D PMVSOH homopolymer and N-H_A-N triblock comicelles, when H_A segments were confined by the two N segments at both ends, this ratio shifted to 5/1. This is presumably due to the existence of the N segments, which partially shielded 2VP groups and resulted in steric hindrance between the triblock comicelles. This steric hindrance prevented the triblock comicelles packing closely, so that an excess of hydroxyl groups, and thus H_D PMVSOH homopolymer, was needed. This can be best appreciated by a comparison of the TEM images shown in Figure S5c, where the seeds were very densely packed in the precipitate to maximize the interaction with H_D PMVSOH homopolymer, and those for "shish-kebab" supermicelles, where two N segments were grown onto the H_A seeds attached to the triblock comicelles, and the intermicellar packing was clearly lower (this is especially clear in the inset image in Figure 1c). Similarly, when H_D segments were confined by N segments and H_A seeds were used, an excess of H_A seeds was required to prevent the intermicellar interaction to form large bundles of triblock comicelles, as shown in Figure S13. This requires that the ratio is further shifted to 1/2 for the formation of composite "shish-kebab" supermicelles from N-H_D-N triblock comicelles and H_A seeds.

DOI: 10.1021/jacs.6b05973
J. Am. Chem. Soc. 2016, 138, 12902−12912

3.2. Formation of "Shish-kebab" Supermicelles. When the H_D homopolymer PMVSOH was added to N-H_A-N triblock comicelles, the PMVSOH chains appeared to function as a "glue" to enable the triblock comicelles to assemble via H-bonding interactions. Meanwhile, the N segments confined the interaction to only the central H_A segments, leading to the formation of colloidally stable supermicelles.

As P2VP chains are soluble in *i*-PrOH and interact with H_D homopolymer, the strength of the H-bonding interaction will increase with the value of DP_{P2VP}, and this effect will promote aggregation of the triblock comicelles to form supermicelles. On the other hand, increasing the DP_{PtBA} block leads to an increased steric effect, hindering triblock comicelle aggregation. By manipulating these factors, different supermicellar aggregates or supermicelles were obtained.

When DP_{P2VP} = 448 and DP_{PtBA} = 170, the steric hindrance was insufficient to confine the H-bonding interactions, and three-dimensional aggregates were formed (Figure 2c and Scheme 2a). When DP_{PtBA} was increased to 280 or 460, the strength of steric hindrance increased and the H-bonding interaction was more confined, and thus "shish-kebab" supermicelles were obtained (Figures 1c and 2b, respectively, and Scheme 2b). However, when DP_{PtBA} was further increased to 600, the steric hindrance was sufficient to partially or even fully shield the central H_A segments from interactions that would cause aggregation, and the block comicelles remained as discrete structures in solution (Figure 2a, Scheme 2c).

Scheme 2. Schematic Illustrations of Different Cases of N-H_A-N Triblock Comicelles: (a) DP_{PtBA} Smaller than DP_{P2VP}; (b) DP_{PtBA} Comparable to DP_{P2VP}; (c) DP_{PtBA} Larger than DP_{P2VP}; and (d) DP_{PtBA} Comparable to DP_{P2VP} and the H_A Segment Is Long[a]

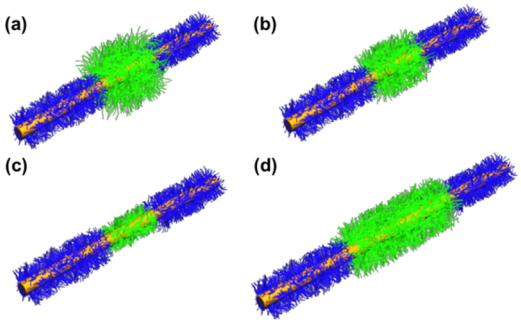

[a]Examples for the cases of (a)−(d) are shown in Figure 2c,f, 2b,e, 2a,d, and 3b,c, respectively.

Increasing the strength of H-bonding interaction (by means of an increase in the value of DP_{P2VP}) had the same effect as decreasing the steric hindrance. As is clear from the TEM analysis, when the strength of the attractive interaction was increased (and DP_{PtBA} was fixed to 280), the aggregation of the micelles was enhanced, and the triblock comicelles formed individual supermicelles (DP_{P2VP} = 250, Figure 2d and Scheme 2c), "shish-kebab" supermicelles (DP_{P2VP} = 448, Figure 2e and Scheme 2b), and three-dimensional aggregates (DP_{P2VP} = 760, Figure 2f and Scheme 2a). The morphologies of these supermicelles or aggregates were very similar to those obtained by varying the DP_{PtBA} value, suggesting that the "shish-kebab" supermicelles result from a delicate balance between attractive interactions (from the H_A segments and H_D PMVSOH homopolymer) and repulsive interactions (from the N segments). Only in cases where both interactions were of comparable strength were triblock comicelles able to form "shish-kebab" supermicelles.

The attractive and repulsive interactions can, in principle, be enhanced by increasing the lengths of the H_A and N segments, respectively. However, as shown in Figure 4 and Figure S11, increasing the length of N segments was not found to significantly influence the morphology of the resultant supermicellar aggregates. This is probably due to the fact that the confinement of H-bonding interactions originates only from the PtBA chains in close proximity to the H_A segments and therefore is only influenced by DP_{PtBA} and not the length of N segments. In contrast, longer H_A segments provide more interacting sites to bind with H_D homopolymer (Scheme 2d), and the enhanced attractive interactions that result lead to the formation of multi-layered bundles (Figure 3).

Finally, "shish-kebab" supermicelles were formed in *i*-PrOH solution, simply by mixing the N-H_A-N triblock and PMVSOH homopolymer together. Although the supermicelle structures were characterized by TEM after they were dried on grids, they were formed in the solution state. The results from our DLS experiments revealed an increase in hydrodynamic diameter from 230 nm for the triblock comicelle N_{280}-$H_{A,448}$(50 nm)-N_{280} (with N segment length = 450 nm) to 615 nm for the "shish-kebab" supermicelles. This result clearly demonstrated that aggregation occurred in the solution state rather than simply on drying during solvent evaporation. This is consistent with the results of LSCFM experiments on the formation of a range of supermicelles utilizing non-covalent interactions,[11e,23] including, for example, complex "windmill" architectures[23] containing H-bonding interactions analogous to those used in the studies reported here.

3.3. Formation of Composite "Shish-kebab" Supermicelles. When H_A seeds were mixed with N-H_D-N triblock comicelles in *i*-PrOH, the seeds were adsorbed onto the central H_D segments due to the strong H-bonding interaction between the P2VP and PMVSOH corona chains. The number of H_A seeds that can be adsorbed onto the triblock comicelles is determined by two factors: the length of H_D segments and the size of the H_A seeds.

As shown in Figure 5, with an increase in DP_{P2VP} for the H_A seeds, the number of seeds that can be adsorbed onto the same N-H_D-N triblock comicelles decreased. In the case of H_D segments with a length of 600 nm, when DP_{P2VP} = 250 (Figure 5a), approximately 30 $H_{A,250}$ seeds can be adsorbed; when DP_{P2VP} = 448 (Figure 5b), the value was ca. 14 $H_{A,448}$ seeds; and when DP_{P2VP} = 760 (Figure 5d), ca. 5 $H_{A,760}$ seeds were adsorbed (in each case the number of adsorbed seeds was counted from TEM images and averaged from more than 40 supermicelles). Thus, the average length of the H_D segment that can be occupied by each H_A seed can be calculated to be 20, 43, and 120 nm, respectively. However, the hydrodynamic diameters of these seeds were measured by DLS to be 58, 72, and 88 nm for $H_{A,250}$, $H_{A,448}$, and $H_{A,760}$, respectively (Figure S15). The trend obtained for the solvated seeds therefore agrees with that calculated from dried samples. However, due to the existence of multiple interacting sites between H_A seeds and H_D segments, the H-bonding interactions may be sufficiently strong to make the adsorption of H_A seeds irreversible. This presumably leads to a non-uniform packing of the H_A seeds on H_D segments, which is particularly clear in Figure 5d. The inefficient packing would also help explain the

DOI: 10.1021/jacs.6b05973
J. Am. Chem. Soc. 2016, 138, 12902−12912

lack of a more quantitative relation between the length of the micelle occupied and the hydrodynamic size of a seed.

As expected, the number of H_A seeds that can be adsorbed is determined by the length of H_D segments. We measured over 300 composite "shish-kebab" supermicelles and plotted the number of H_A seeds versus the length of H_D segments in Figure 9a. From the plot, it is clear that the number of H_A seeds is proportional to the length of H_D segments. From the slope, the average length occupied by each $H_{A,448}$ seed can be calculated to be 38 nm. However, if N-H_D-N triblock comicelles with a short H_D segment were used, only when the H_D segment was at least 80 nm long could the H_A seeds be adsorbed effectively. Furthermore, instead of forming a one-to-one complex, two seeds were adsorbed onto each of the triblock comicelles. This could be explained by the fact that the H_D segments were surrounded by PtBA chains, which can partially shield the H-bonding interaction, as shown in Scheme 3a. It is likely that the

Scheme 3. Schematic Illustration of the Factors Influencing the H-Bonding Interactions of N-H_D-N Triblock Comicelles: (a) for a Short H_D Segment (for Example, for the Comicelles Shown in Figures 9 and S20) and (b) for a Long H_D Segment (for Example, for the Comicelles Shown in Figures 5 and 6)

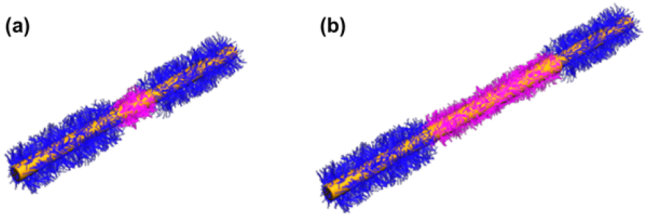

H_D segments need to reach a minimum length to adsorb H_A seeds and overcome the ability of the PtBA chains to effectively prevent H-bonding interactions (Scheme 3b). However, once the minimum length has been achieved, even if the corona chains are short (DP of PMVSOH is only 120), the H_D segments still exist in three dimensions, and the seeds can then be adsorbed from different directions.

Significantly, the H_A seeds adsorbed onto the triblock comicelles remained active for further living CDSA, and addition of the PFS-*b*-PtBA unimer led to the formation of N segments and thus fence-like "shish-kebab" supermicelles. The number of N segments that can be grown is determined by the number of seeds adsorbed and thus, as discussed in the previous section, the length of H_D segments. On the other hand, the region where seeds can be adsorbed is determined by the position of the H_D segments. Therefore, by careful design of the H_D segment-containing block comicelles, we could produce fence-like "shish-kebab" supermicelles (Figure 7) or even block fence-like "shish-kebab" supermicelles (Figure 8).

4. SUMMARY

We report an in-depth study of the hierarchical assembly of BCP micelles into complex higher-level structures via the use of H-bonding interactions. Virtually monodisperse cylindrical block comicelles bearing H-bonding central segments (with either donor H_D or acceptor H_A coronal functionality) and non-interactive end segments (N) were prepared via living CDSA. The lengths and the locations of these segments were precisely controlled. The cylindrical block comicelles were assembled in *i*-PrOH via H-bonding interactions, and various interesting and complex supermicellar structures were obtained. We focused on the formation of "shish-kebab" supermicelles from N-H_A-N triblock comicelles and the H_D-based homopolymer, or N-H_D-N triblock comicelles and H_A seeds, and, in the latter case, the resulting fence-like "shish-kebab" supermicelles. Their formation can be rationalized by the influence of two factors: attractive H-bonding interactions between the P2VP and PMVSOH chains, and unfavorable steric repulsions from the non-interacting PtBA chains. The resulting structures were found to be stable in solution over several months under ambient conditions based on TEM analysis. Moreover, they are anticipated to be "static", kinetically trapped assemblies rather than "dynamic" structures with respect to unimer exchange based on our previous results on fluorescently labeled supermicelles constructed using similar H-bonding interactions.[23]

Although the methodology described here was based on PFS-containing BCPs, it should be applicable to the emerging group of other crystalline-coil BCPs and related molecular species that undergo seeded growth processes analogous to living CDSA.[18−20] This study demonstrates avenues with which to construct new micrometer-scale supermicellar structures via hydrogen bonding. In principle, functional structures may be generated by taking advantage of the tailorable spatial organization of different coronal chemistries. This may provide a powerful method for the preparation of complex micrometer-scale structures with a variety of applications.

■ ASSOCIATED CONTENT

Supporting Information

The Supporting Information is available free of charge on the ACS Publications website at DOI: 10.1021/jacs.6b05973.

Experimental details and additional results (PDF)

■ AUTHOR INFORMATION

Corresponding Author

*ian.manners@bristol.ac.uk

Present Address

[‖]X.L.: Department of Polymer Materials, School of Material Science and Technology, Beijing Institute of Technology, Beijing 100081, P.R. China

Author Contributions

[§]X.L. and Y.G. contributed equally.

Notes

The authors declare no competing financial interest.

■ ACKNOWLEDGMENTS

X.L. acknowledges the EU for a Marie Curie Postdoctoral Fellowship. Y.G. and I.M. thank the EU for support. M.W. thanks the Natural Sciences and Engineering Research Council of Canada for financial support. I.M. also thanks EPSRC for support. We also thank the Wolfson Bioimaging Facility at the University of Bristol for the use of the confocal microscopy facilities. PeakForce atomic force microscopy was carried out in the Chemical Imaging Facility, University of Bristol, with equipment funded by EPSRC (EP/K035746/1). TEM studies were carried out in the Chemistry Imaging Facility at UoB with equipment funded by UoB and EPSRC (EP/K035746/1 and EP/M028216/1).

DOI: 10.1021/jacs.6b05973
J. Am. Chem. Soc. 2016, 138, 12902−12912

REFERENCES

(1) Fratzl, P.; Weinkamer, R. *Prog. Mater. Sci.* **2007**, *52*, 1263−1334.
(2) Pabo, C. O.; Sauer, R. T. *Annu. Rev. Biochem.* **1984**, *53*, 293−321.
(3) Dobson, C. M. *Nature* **2003**, *426*, 884−890.
(4) Whitesides, G. M.; Grzybowski, B. *Science* **2002**, *295*, 2418−2421.
(5) (a) Douglas, S. M.; Dietz, H.; Liedl, T.; Hoegberg, B.; Graf, F.; Shih, W. M. *Nature* **2009**, *459*, 414−418. (b) Winfree, E.; Liu, F. R.; Wenzler, L. A.; Seeman, N. C. *Nature* **1998**, *394*, 539−544. (c) Goodman, R. P.; Schaap, I. A. T.; Tardin, C. F.; Erben, C. M.; Berry, R. M.; Schmidt, C. F.; Turberfield, A. J. *Science* **2005**, *310*, 1661−1665. (d) Lo, P. K.; Karam, P.; Aldaye, F. A.; McLaughlin, C. K.; Hamblin, G. D.; Cosa, G.; Sleiman, H. F. *Nat. Chem.* **2010**, *2*, 319−328. (e) He, Y.; Ye, T.; Su, M.; Zhang, C.; Ribbe, A. E.; Jiang, W.; Mao, C. D. *Nature* **2008**, *452*, 198−U141.
(6) (a) Prins, L. J.; De Jong, F.; Timmerman, P.; Reinhoudt, D. N. *Nature* **2000**, *408*, 181−184. (b) Prins, L. J.; Huskens, J.; de Jong, F.; Timmerman, P.; Reinhoudt, D. N. *Nature* **1999**, *398*, 498−502. (c) Hirschberg, J.; Brunsveld, L.; Ramzi, A.; Vekemans, J.; Sijbesma, R. P.; Meijer, E. W. *Nature* **2000**, *407*, 167−170. (d) Hartgerink, J. D.; Beniash, E.; Stupp, S. I. *Science* **2001**, *294*, 1684−1688. (e) Brunsveld, L.; Vekemans, J.; Hirschberg, J.; Sijbesma, R. P.; Meijer, E. W. *Proc. Natl. Acad. Sci. U. S. A.* **2002**, *99*, 4977−4982.
(7) (a) Ruokolainen, J.; Makinen, R.; Torkkeli, M.; Makela, T.; Serimaa, R.; ten Brinke, G.; Ikkala, O. *Science* **1998**, *280*, 557−560. (b) Valkama, S.; Kosonen, H.; Ruokolainen, J.; Haatainen, T.; Torkkeli, M.; Serimaa, R.; Ten Brinke, G.; Ikkala, O. *Nat. Mater.* **2004**, *3*, 872−876. (c) Zhao, Y.; Thorkelsson, K.; Mastroianni, A. J.; Schilling, T.; Luther, J. M.; Rancatore, B. J.; Matsunaga, K.; Jinnai, H.; Wu, Y.; Poulsen, D.; Fréchet, J. M. J.; Alivisatos, A. P.; Xu, T. *Nat. Mater.* **2009**, *8*, 979−985.
(8) Tang, C. B.; Lennon, E. M.; Fredrickson, G. H.; Kramer, E. J.; Hawker, C. J. *Science* **2008**, *322*, 429−432.
(9) (a) Zhang, L. F.; Eisenberg, A. *Science* **1995**, *268*, 1728−1731. (b) Zhang, L. F.; Yu, K.; Eisenberg, A. *Science* **1996**, *272*, 1777−1779. (c) Gröschel, A. H.; Walther, A.; Löbling, T. I.; Schacher, F. H.; Schmalz, H.; Müller, A. H. E. *Nature* **2013**, *503*, 247−251. (d) Gröschel, A. H.; Schacher, F. H.; Schmalz, H.; Borisov, O. V.; Zhulina, E. B.; Walther, A.; Müller, A. H. E. *Nat. Commun.* **2012**, *3*, 710. (e) Li, Z. B.; Kesselman, E.; Talmon, Y.; Hillmyer, M. A.; Lodge, T. P. *Science* **2004**, *306*, 98−101. (f) Zhu, J.; Zhang, S.; Zhang, K.; Wang, X.; Mays, J. W.; Wooley, K. L.; Pochan, D. J. *Nat. Comm.* **2013**, *4*, 2297. (g) Cui, H.; Chen, Z.; Zhong, S.; Wooley, K. L.; Pochan, D. J. *Science* **2007**, *317*, 647−650. (h) Pochan, D. J.; Chen, Z. Y.; Cui, H. G.; Hales, K.; Qi, K.; Wooley, K. L. *Science* **2004**, *306*, 94−97. (i) Cheng, C.; Qi, K.; Khoshdel, E.; Wooley, K. L. *J. Am. Chem. Soc.* **2006**, *128*, 6808−6809. (j) Dupont, J.; Liu, G.; Niihara, K.; Kimoto, R.; Jinnai, H. *Angew. Chem., Int. Ed.* **2009**, *48*, 6144−6147. (k) Li, Z.; Ma, J.; Lee, N. S.; Wooley, K. L. *J. Am. Chem. Soc.* **2011**, *133*, 1228−1231. (l) Walther, A.; Andre, X.; Drechsler, M.; Abetz, V.; Müller, A. H. E. *J. Am. Chem. Soc.* **2007**, *129*, 6187−6198.
(10) (a) Zhang, K.; Fang, H. F.; Li, Z.; Ma, J.; Hohlbauch, S. V.; Taylor, J.-S. A.; Wooley, K. L. *Soft Matter* **2009**, *5*, 3585−3589. (b) Shrestha, R.; Elsabahy, M.; Luehmann, H.; Samarajeewa, S.; Florez-Malaver, S.; Lee, N. S.; Welch, M. J.; Liu, Y. J.; Wooley, K. L. *J. Am. Chem. Soc.* **2012**, *134*, 17362−17365. (c) Li, X. Y.; Liu, G.; Han, D. *Soft Matter* **2011**, *7*, 8216−8223. (d) Liu, C.; Zhang, K.; Chen, D. Y.; Jiang, M.; Liu, S. Y. *Chem. Commun.* **2010**, *46*, 6135−6137. (e) Schacher, F.; Betthausen, E.; Walther, A.; Schmalz, H.; Pergushov, D. V.; Müller, A. H. E. *ACS Nano* **2009**, *3*, 2095−2102.
(11) (a) Li, X. Y.; Gao, Y.; Boott, C. E.; Hayward, D. W.; Harniman, R.; Whittell, G. R.; Richardson, R. M.; Winnik, M. A.; Manners, I. *J. Am. Chem. Soc.* **2016**, *138*, 4087−4095. (b) Abbas, S.; Li, Z.; Hassan, H.; Lodge, T. P. *Macromolecules* **2007**, *40*, 4048−4052. (c) Walther, A.; Drechsler, M.; Rosenfeldt, S.; Harnau, L.; Ballauff, M.; Abetz, V.; Müller, A. H. E. *J. Am. Chem. Soc.* **2009**, *131*, 4720−4728. (d) Cheng, L.; Zhang, G.; Zhu, L.; Chen, D.; Jiang, M. *Angew. Chem., Int. Ed.* **2008**, *47*, 10171−10174. (e) Qiu, H.; Hudson, Z. M.; Winnik, M. A.; Manners, I. *Science* **2015**, *347*, 1329−1332.
(12) O'Leary, L. E. R.; Fallas, J. A.; Bakota, E. L.; Kang, M. K.; Hartgerink, J. D. *Nat. Chem.* **2011**, *3*, 821−828.
(13) (a) Gädt, T.; Ieong, N. S.; Cambridge, G.; Winnik, M. A.; Manners, I. *Nat. Mater.* **2009**, *8*, 144−150. (b) Wang, X.; Guérin, G.; Wang, H.; Wang, Y.; Manners, I.; Winnik, M. A. *Science* **2007**, *317*, 644−647.
(14) Gilroy, J. B.; Gädt, T.; Whittell, G. R.; Chabanne, L.; Mitchels, J. M.; Richardson, R. M.; Winnik, M. A.; Manners, I. *Nat. Chem.* **2010**, *2*, 566−570.
(15) (a) He, F.; Gädt, T.; Manners, I.; Winnik, M. A. *J. Am. Chem. Soc.* **2011**, *133*, 9095−9103. (b) Hudson, Z. M.; Lunn, D. J.; Winnik, M. A.; Manners, I. *Nat. Commun.* **2014**, *5*, 3372.
(16) Qiu, H.; Cambridge, G.; Winnik, M. A.; Manners, I. *J. Am. Chem. Soc.* **2013**, *135*, 12180−12183.
(17) Rupar, P. A.; Chabanne, L.; Winnik, M. A.; Manners, I. *Science* **2012**, *337*, 559−562.
(18) (a) Petzetakis, N.; Dove, A. P.; O'Reilly, R. K. *Chem. Sci.* **2011**, *2*, 955−960. (b) Sun, L.; Petzetakis, N.; Pitto-Barry, A.; Schiller, T. L.; Kirby, N.; Keddie, D. J.; Boyd, B. J.; O'Reilly, R. K.; Dove, A. P. *Macromolecules* **2013**, *46*, 9074−9082. (c) Sun, L.; Pitto-Barry, A.; Kirby, N.; Schiller, T. L.; Sanchez, A. M.; Dyson, M. A.; Sloan, J.; Wilson, N. R.; O'Reilly, R. K.; Dove, A. P. *Nat. Commun.* **2014**, *5*, 5746.
(19) (a) Lee, I.-H.; Amaladass, P.; Yoon, K.-Y.; Shin, S.; Kim, Y.-J.; Kim, I.; Lee, E.; Choi, T.-L. *J. Am. Chem. Soc.* **2013**, *135*, 17695−17698. (b) Qian, J.; Li, X. Y.; Lunn, D. J.; Gwyther, J.; Hudson, Z. M.; Kynaston, E.; Rupar, P. A.; Winnik, M. A.; Manners, I. *J. Am. Chem. Soc.* **2014**, *136*, 4121−4124. (c) Patra, S. K.; Ahmed, R.; Whittell, G. R.; Lunn, D. J.; Dunphy, E. L.; Winnik, M. A.; Manners, I. *J. Am. Chem. Soc.* **2011**, *133*, 8842−8845. (d) Kamps, A. C.; Fryd, M.; Park, S.-J. *ACS Nano* **2012**, *6*, 2844−2852.
(20) (a) Schmelz, J.; Schedl, A. E.; Steinlein, C.; Manners, I.; Schmalz, H. *J. Am. Chem. Soc.* **2012**, *134*, 14217−14225. (b) Schmalz, H.; Schmelz, J.; Drechsler, M.; Yuan, J.; Walther, A.; Schweimer, K.; Mihut, A. M. *Macromolecules* **2008**, *41*, 3235−3242. (c) Schmelz, J.; Schacher, F. H.; Schmalz, H. *Soft Matter* **2013**, *9*, 2101−2107. (d) Schöbel, J.; Karg, M.; Rosenbach, D.; Krauss, G.; Greiner, A.; Schmalz, H. *Macromolecules* **2016**, *49*, 2761−2771.
(21) (a) Hudson, Z. M.; Boott, C. E.; Robinson, M. E.; Rupar, P. A.; Winnik, M. A.; Manners, I. *Nat. Chem.* **2014**, *6*, 893−898. (b) Qiu, H.; Gao, Y.; Boott, C.; Gould, O. E. C.; Harniman, R. L.; Webb, S. E. D.; Winnik, M. A.; Manners, I. *Science* **2016**, *352*, 697−701.
(22) (a) Qiu, H.; Russo, G.; Rupar, P. A.; Chabanne, L.; Winnik, M. A.; Manners, I. *Angew. Chem., Int. Ed.* **2012**, *51*, 11882−11885. (b) Li, X.; Gao, Y.; Boott, C. E.; Hayward, D. W.; Harniman, R.; Whittell, G. R.; Richardson, R. M.; Winnik, M. A.; Manners, I. *J. Am. Chem. Soc.* **2016**, *138*, 4087−4095.
(23) Li, X. Y.; Gao, Y.; Boott, C. E.; Winnik, A. M.; Manners, I. *Nat. Commun.* **2015**, *6*, 8127.
(24) (a) Ni, Y. Z.; Rulkens, R.; Manners, I. *J. Am. Chem. Soc.* **1996**, *118*, 4102−4114. (b) McGrath, N.; Schacher, F. H.; Qiu, H.; Mann, S.; Winnik, M. A.; Manners, I. *Polym. Chem.* **2014**, *5*, 1923−1929. (c) Hailes, R. L. N.; Oliver, A. M.; Gwyther, J.; Whittell, G. R.; Manners, I. *Chem. Soc. Rev.* **2016**, DOI: 10.1039/c6cs00155f.
(25) (a) Gilroy, J. B.; Rupar, P. A.; Whittell, G. R.; Chabanne, L.; Terrill, N. J.; Winnik, M. A.; Manners, I.; Richardson, R. M. *J. Am. Chem. Soc.* **2011**, *133*, 17056−17062. (b) Lammertink, R. G. H.; Hempenius, M. A.; Manners, I.; Vancso, G. J. *Macromolecules* **1998**, *31*, 795−800. (c) Papkov, V. S.; Gerasimov, M. V.; Dubovik, II; Sharma, S.; Dementiev, V. V.; Pannell, K. H. *Macromolecules* **2000**, *33*, 7107−7115. (d) Chen, Z. H.; Foster, M. D.; Zhou, W. S.; Fong, H.; Reneker, D. H.; Resendes, R.; Manners, I. *Macromolecules* **2001**, *34*, 6156−6158.
(26) Lunn, D. J.; Boott, C. E.; Bass, K. E.; Shuttleworth, T. A.; McCreanor, N. G.; Papadouli, S.; Manners, I. *Macromol. Chem. Phys.* **2013**, *214*, 2813−2820.
(27) (a) Chen, D. Y.; Jiang, M. *Acc. Chem. Res.* **2005**, *38*, 494−502. (b) Jiang, M.; Li, M.; Xiang, M. L.; Zhou, H. In *Polymer Synthesis Polymer−Polymer Complexation*; Abe, A., Albertsson, A. C., Cantow, H. J., Dusek, K., Edwards, S., Hocker, H., Joanny, J. F., Kausch, H. H.,

DOI: 10.1021/jacs.6b05973
J. Am. Chem. Soc. 2016, 138, 12902−12912

Kobayashi, T., Lee, K. S., McGarth, J. E., Monnerie, L., Stupp, S. I., Suter, U. W., Thomas, E. L., Wegner, G., Young, R. J., Eds.; Advances in Polymer Science *146*; Springer: Berlin/Heidelberg, 1999; pp 121−196.
(28) Liu, S. Y.; Zhu, H.; Zhao, H. Y.; Jiang, M.; Wu, C. *Langmuir* **2000**, *16*, 3712−3717.
(29) Jia, L.; Zhao, G.; Shi, W.; Coombs, N.; Gourevich, I.; Walker, G. C.; Guerin, G.; Manners, I.; Winnik, M. A. *Nat. Commun.* **2014**, *5*, 3882.

DOI: 10.1021/jacs.6b05973
J. Am. Chem. Soc. 2016, 138, 12902−12912